Proc. Natl. Acad. Sci. USA
Vol. 85, pp. 2412–2416, April 1988
Physiological Sciences

Ca channels in adrenal glomerulosa cells: K^+ and angiotensin II increase T-type Ca channel current

(stimulus–secretion coupling/nitrendipine/aldosterone)

CHARLES J. COHEN*†, RICHARD T. MCCARTHY*, PAULA Q. BARRETT‡, AND HOWARD RASMUSSEN‡

*Miles Institute for Preclinical Pharmacology, New Haven, CT 06509; and ‡Department of Medicine, Yale University School of Medicine, New Haven, CT 06510

Communicated by Gerhard Giebisch, December 8, 1987 (received for review July 7, 1987)

ABSTRACT **Ca channel currents were studied in freshly dispersed bovine adrenal glomerulosa cells to better understand the control of aldosterone secretion by extracellular K concentration (K_o) and angiotensin II (AII). The whole-cell variation of the patch voltage clamp technique was used. Two types of Ca channels were found. One type is similar to the "T-type" Ca channels found in many excitable cells. These channels deactivate slowly ($\tau \approx 7$ ms at -75 mV) and inactivate rapidly during strong depolarizations. The second channel type activates and inactivates at more positive potentials than the T-type Ca channels and deactivates rapidly. These channels are similar to the "L-type" Ca channels found in muscle and nerve. Our studies provide three reasons for concluding that T-type Ca channels have an important role in mediating stimulus–secretion coupling in response to high K^+ or AII: (*i*) aldosterone secretion and steady-state current through T-type Ca channels are biphasic functions of K_o and both increase in parallel for K_o = 2–10 mM; (*ii*) nitrendipine blocks the T-type Ca channels and the stimulation of aldosterone secretion by high K^+ or AII with similar potency; (*iii*) AII increases Ca entry through the T-type Ca channels.**

The principal mechanism for regulating plasma K^+ concentration in mammals involves the secretion of aldosterone from adrenal glomerulosa cells. This mechanism is efficacious because small changes in plasma K^+ result in large parallel changes in aldosterone secretion. Stimulus–secretion coupling is thought to be mediated by voltage-gated Ca channels because small changes in extracellular K concentration (K_o) (≈2–10 mM) depolarize the cell membrane and cause an increase in the influx of ^{45}Ca that can be inhibited by the Ca channel blocker nitrendipine or its congeners (1–13). Electrophysiological studies with vascular smooth muscle and other tissues have shown that ^{45}Ca influx that is stimulated by high K^+ and blocked by nitrendipine represents Ca entry through voltage-gated channels (14–17). However, no comparable studies have been performed with adrenal glomerulosa cells and the effects of high K^+ and nitrendipine on these cells differ in several significant ways from previously studied tissues.

Aldosterone secretion is a biphasic function of K_o; secretion increases with K_o up to 10–12 mM, but further increases in K_o cause a drop in secretion and in intracellular Ca^{2+} (1–4, 13). In contrast, the physiological response increases monotonically with K_o over a broad concentration range in most other types of secretory cells and smooth muscle, and much higher K_o are necessary to evoke a significant response. Likewise, Ca influx increases over a broad voltage range in previously studied cells. High-affinity binding of [^3H]nitrendipine to adrenal glomerulosa cells is similar to that for other tissues (4, 18), but the IC_{50} for nitrendipine block of K^+-induced Ca influx in adrenal glomerulosa cells is ≈100-fold greater than for smooth muscle or some other secretory cells and ≈1000-fold greater than the K_d for high-affinity ligand binding (1, 4).

Stimulation of aldosterone secretion by angiotensin II (AII) involves two changes in cellular Ca^{2+} metabolism: Ca^{2+} is released from intracellular stores by way of inositol 1,4,5-trisphosphate and Ca^{2+} influx across the plasmalemma is increased in a sustained manner (2, 3, 12, 13, 19-21). Although it is clear that the increase in Ca^{2+} influx mediates the sustained effects of AII, the nature of the Ca influx pathway is not defined (3).

We have used the patch electrode voltage clamp technique to better define the role of Ca channels in stimulus–secretion coupling in adrenal glomerulosa cells. Two questions were addressed: (*i*) Can the unusual dependence of Ca^{2+} influx on K_o be accounted for by the voltage dependence of Ca channel gating? (*ii*) Does AII stimulate Ca^{2+} influx by increasing Ca^{2+} entry through voltage-gated Ca channels? A preliminary report of this work has been published (22).

MATERIALS AND METHODS

Bovine adrenal glomerulosa cells were prepared by collagenase digestion (20). Cells were stored at 0°C in physiological saline for 1–5 hr before use. The bath solution used for recording Ca channel currents contained (in mM) tetraethylammonium chloride, 117; $BaCl_2$, 20; $MgCl_2$, 0.5; dextrose, 5; sucrose, 32; Hepes, 10; and tetrodotoxin, 2×10^{-4}; pH 7.5 (adjusted with CsOH). Bath solutions were gassed with 100% oxygen and maintained at room temperature (20–24°C). The patch pipettes were filled with a solution that contained (in mM) CsCl, 108; tetrabutylammonium chloride, 10; bis(2-aminophenoxy)ethane-*N*,*N*,*N*′,*N*′-tetraacetate (BAPTA), 11; $CaCl_2$, 0.9; $MgCl_2$, 6; Na_2ATP, 5; GTP, 0.04; and Hepes, 20; pH 7.2 (adjusted with CsOH). Nitrendipine and nimodipine were synthesized by Bayer AG (Wuppertal, F.R.G.) and stored as 1 mM stock solutions in polyethylene glycol 400. AII was obtained from Sigma.

Ca channel currents were studied by using the whole-cell variation of the patch electrode voltage clamp technique (23) as described (16). Membrane current was sampled at 10 or 20 kHz and filtered with an 8-pole low-pass Bessel filter with a cut-off frequency (−3 decibel) of 2.5 or 5 kHz, respectively. Linear leak and capacity currents were subtracted digitally by appropriately scaling a test pulse from −90 to −110 mV. When tail currents consisted of two exponential components, an exponential was fit to the slow component and was digitally subtracted from the total tail current. The remainder

The publication costs of this article were defrayed in part by page charge payment. This article must therefore be hereby marked "*advertisement*" in accordance with 18 U.S.C. §1734 solely to indicate this fact.

Abbreviations: AII, angiotensin II; K_o, extracellular K concentration.

†To whom reprint request should be addressed at: Merck Sharp & Dohme Research Laboratories, P.O. Box 2000, Room 80L-106, Rahway, NJ 07065.

was then fit with an exponential. Nonlinear least squares curve fitting was performed by using the Patternsearch algorithm (24).

RESULTS

Bovine Adrenal Glomerulosa Cells Have Two Types of Ca Channels. Fig. 1 shows the voltage dependence of activation of Ca channels in glomerulosa cells and presents evidence for two distinct types of Ca channels in these cells. Fig. 1 *Top* shows superimposed measurements of Ca channel currents elicited during test pulses to −30, 0, and +30 mV and after repolarization. The Ca channel currents during each test pulse were quite small. This cell was typical of all of our experiments, in that we rarely measured inward currents >30 pA with 20 mM Ba as the charge carrier. Since the leak currents elicited by the test pulses were comparable in magnitude to the Ca channel currents, it was difficult to quantitate the Ca channel currents during the test pulse. However, repolarization of the membrane potential to ≤−65 mV always revealed a slowly deactivating tail current that increased in amplitude as the preceding test potential (V_t) became more positive. The tail currents could usually be fit by a single exponential. The amplitude of this exponential indicated the instantaneous conductance of these Ca channels at the time of repolarization. The relative amplitude of this tail current is plotted vs. V_t in Fig. 1 *Bottom* (open squares). Each datum point represents the mean of three experiments. The solid curve through these data is a nonlinear least squares fit to the equation $I/I_{max} = \{1 + \exp[(V_d - V_t)/k]\}^{-1}$, with $V_d = -7.1$ mV and $k = 15.4$.

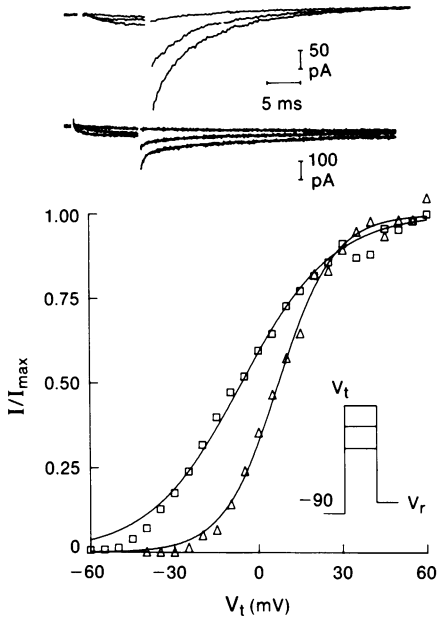

FIG. 1. Bovine adrenal glomerulosa cells have two components of tail current through Ca channels that differ in the voltage dependence of activation. (*Top*) Superimposed current measurements made when the membrane was repolarized to $V_r = -65$ mV. The tail currents decayed exponentially with a time constant of 7.0 ms. (*Middle*) Superimposed current measurements made in a different cell when $V_r = -35$ mV. The tail currents were biexponential and the time constants of decay were 32 and 1.2 ms. Each current record in the *Top* does not include measurements made for 800 μs after changing the membrane potential and those in the *Middle* contain 400-μs gaps. (*Bottom*) Relative amplitude of each component of tail current vs. V_t. The pulse protocol is shown in the *Inset*. The slow component of tail current was measured at −75 mV and the fast component was measured at −35 mV. The test pulse duration was 40 ms for $V_t < 0$ mV and 10 ms for $V_t \geq 0$ mV.

In about 20% of the cells, we found a second component of tail current when the membrane was repolarized to less negative potentials. This component of tail current can be seen in Fig. 1 *Middle*. The current measurements shown are for $V_t = -30$, 0, and +30 mV and the tail currents were measured at −35 mV. Tail currents decay more slowly at this potential and a second exponential component that decays with a time constant of 1.0 ms could now be resolved. The relative amplitude of the rapidly deactivating component of tail current is plotted as a function of V_t in Fig. 1 *Bottom* (open triangles). Each datum point represents the mean result for three experiments. The solid curve through these data is for $V_d = +7.2$ mV and $k = 9.98$. Hence, the rapidly deactivating component of tail current activates at more positive potentials than the slowly deactivating component of tail current.

Two similar components of tail current have been characterized in anterior pituitary cells, sensory neurons, and cell lines derived from vascular smooth muscle (16, 17, 25-27). Those results were most readily explained by invoking two populations of Ca channels. The slowly deactivating Ca channel currents are through "transient" or "T-type" Ca channels that inactivate rapidly during strong depolarizations and are only available for opening when the cell is very well polarized. The rapidly deactivating currents are due to a population of "slowly inactivating" or "L-type" Ca channels that activate and inactivate at more positive potentials. Fig. 2 shows that the same interpretation of the tail current measurements is appropriate to adrenal glomerulosa cells.

Fig. 2*A* shows that the two components of tail current differ in the voltage dependence of steady-state inactivation. The pulse protocol is shown in the *Inset*. The relative amplitude of each component of tail current is plotted vs. V_p. The solid curve through each data set is defined by the equation $I/I_{max} = \{1 + \exp[(V_p - V_h)/k]\}^{-1}$. The slowly deactivating current component (indicated with open squares) is fit with $V_h = -56.1$ mV and $k = 6.68$. The rapidly deactivating current component is fit with $V_h = -40.6$ mV and $k = 9.49$.

Fig. 2*B* shows that the slowly deactivating Ca channels inactivate rapidly during strong depolarizations. The pulse protocol is shown in the *Inset*, and the graph shows a plot of the amplitude of the slow component of tail current as a function of te· pulse duration. The conditions were chosen to minimize Ca-i ıduced inactivation: Ba was the charge carrier,

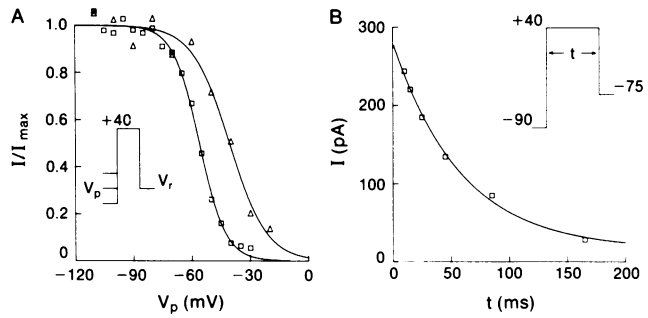

FIG. 2. (*A*) The two components of tail current through Ca channels differ in the voltage dependence of steady-state inactivation. The relative amplitude of each component of tail current is plotted vs. V_p. The solid curve through each set of data points indicates a least squares fit to a two-state Boltzmann distribution. (*B*) The slowly deactivating Ca channels inactivate rapidly during strong depolarizations. The amplitude of the slowly deactivating Ca channel current is plotted vs. the test pulse duration (t). Each tail current measurement was fit by an exponential with a time constant of 6.1 ± 0.2 ms. The solid curve through the data is a least squares fit to $I = (I_0 - I_\infty)\exp(-t/\tau) + I_\infty$ with $I_0 = 281.4$ pA, $I_\infty = 15.8$ pA, and $\tau = 58.2$ ms.

cytoplasmic Ca was buffered at ≈10 mM by 11 mM bis(2-aminophenoxy)ethane-*N*,*N*,*N'*,*N'*-tetraacetate (BAPTA), and the test potential was chosen to be very positive so that there was little inward current during the test pulse. The rapid inactivation is therefore attributable to a voltage-dependent "gate." Hence, the slowly deactivating Ca channels in adrenal glomerulosa cells are similar to the T-type Ca channels found in some types of excitable cells (16, 25–35).

The two components of tail current also differ in their sensitivity to dihydropyridine Ca channel agonists and in their susceptibility to wash out during intracellular dialysis. Addition of 200 nM of the (−)-(4*S*) enantiomer of BAY K 8644 had no effect on the slow component of tail current, but it slowed the rate of deactivation of the fast component and increased its amplitude (data not shown). These effects are similar to those in other cell types in which L-type Ca channels are affected by BAY K 8644 and T-type Ca channels are not (28, 31, 32, 34). The fast component of tail current washed out within 10 min of dialysis by the patch pipette solution, but the slow component was stable. In anterior pituitary cells and sensory neurons, similar observations were best explained by invoking two types of Ca channels (25–27, 33).

High K^+ and AII Increase T-Type Ca Channel Currents. The data in Fig. 3 present evidence that high K^+ stimulates steady-state Ca influx through T-type Ca channels in adrenal glomerulosa cells. Fig. 3*A* shows the voltage dependence of activation and inactivation of the T-type Ca channels, determined by using the same pulse protocols as for Figs. 1 and 2, but each set of data points represents the mean result for three or four experiments. The curve describing the voltage dependence of activation was drawn by assuming second-order activation kinetics: $I/I_{max} = \{1 + \exp[(V_d - V_t)/k]\}^{-2}$. This function gave a better fit to the data for $V_t < -30$ mV than first-order activation kinetics (compare the fit of the curves in Figs. 1 and 3*A*). The important point here is that the curves describing steady-state activation and inactivation overlap. In the voltage range spanned by the overlap, there should be steady-state current through the T-type Ca channels. Fig. 3*B* shows that the voltage dependence of steady-state Ca^{2+} influx through T-type Ca channels can account for the biphasic dependence of aldosterone secretion on K_o. The solid curve is the predicted current through T-type Ca channels based on the curves in Fig. 3*A*. The open triangles indicate the effect of K_o on the influx of ^{45}Ca and we have assumed that the effect of changing K_o is solely on the membrane potential, with the membrane potential at each K_o being estimated with the Goldman–Hodgkin–Katz equation (7). Likewise, the open squares indicate the dependence of aldosterone secretion on K_o. Both sets of data are reproduced from earlier studies from this laboratory, which established that K^+-stimulated aldosterone secretion is proportional to K^+-stimulated Ca^{2+} influx (1, 2). These data suggest that Ca channel currents mediate stimulus–secretion coupling. The voltage clamp studies suggest that aldosterone secretion is stimulated by small increases in K_o because there is steady-state Ca influx through T-type Ca channels that activates at relatively negative potentials. Secretion declines as K_o increases beyond 10–12 mM because steady-state Ca influx does not increase monotonically with voltage.

A second line of evidence indicating that K^+-induced aldosterone secretion is dependent upon Ca^{2+} entry through

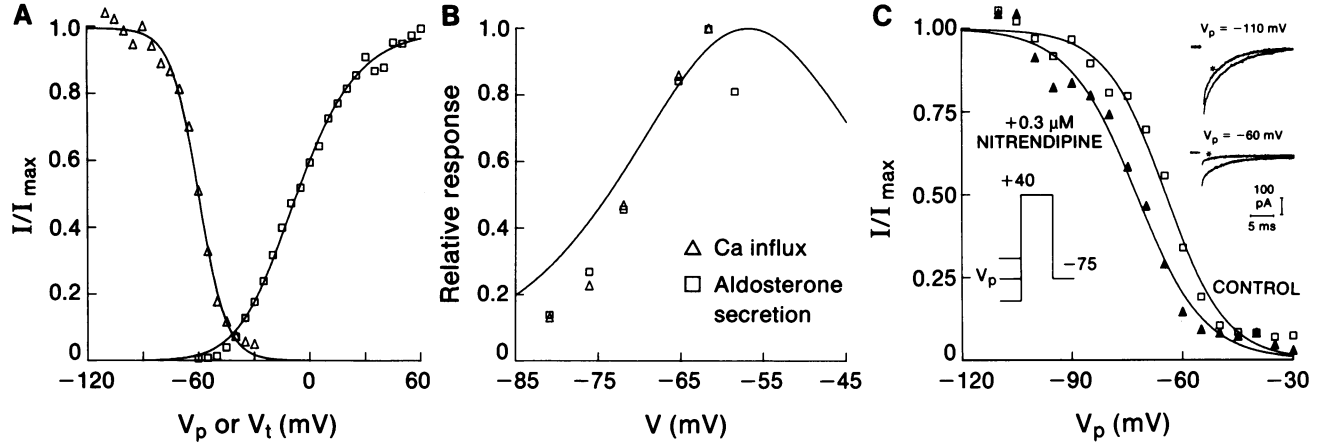

FIG. 3. K^+-stimulated Ca influx is through T-type Ca channels. (*A*) Voltage dependence of activation and inactivation of the T-type Ca channels. Open squares indicate the same data as in Fig. 1. The solid curve through the data is a nonlinear least squares fit to the equation $m_\infty^2 = I/I_{max} = \{1 + \exp[(V_d - V_t)/k]\}^{-2}$, with $V_d = -24.0$ mV and $k = 19.0$. Open triangles indicate the relative amplitude of the slow component of tail current as a function of V_p. Each point represents the mean of four experiments. The solid curve through these data is a least squares fit to the equation $h_\infty = I/I_{max} = \{1 + \exp[(V_p - V_h)/k]\}^{-1}$, with $V_h = -59.8$ mV and $k = 7.27$. (*B*) Voltage dependence of ^{45}Ca influx, aldosterone secretion, and steady-state current through the T-type Ca channels. Note that the abscissa differs from that in *A*. The solid curve indicates the predicted steady-state current through the T-type Ca channels (I_∞) and is given by $I_\infty = \bar{g}_{Ca} m_\infty^2 h_\infty (V_{rev} - V)$, where m_∞ and h_∞ are defined above, $\bar{g}_{Ca}$ is the maximal conductance of the T-type Ca channels and was chosen so that the maximal value of I_∞ is 1.0, and V_{rev} is the reversal potential for the T-type Ca channels. The curve assumes that $V_{rev} = +70$ mV, but the shape of the curve is little affected by varying V_{rev} from +30 to +110 mV. Open squares indicate the relative levels of aldosterone secretion for K_o = 2, 3.5, 5, 8, 10, and 12 mM. Each value of K_o has been converted to an equivalent membrane potential by assuming the validity of the Goldman–Hodgkin–Katz equation: $V = (RT/F)\ln\{[K_o + (P_{Na}/P_K)Na_o]/K_i\} = (61)\log\{[K_o + (0.037)(150)]/160\}$, where P_{Na}/P_K is the permeability of Na relative to the permeability of K, and K_i is the intracellular concentration of K. This equation is known to be valid for rat adrenal glomerulosa cells (7). P_{Na}/P_K was chosen so that $V = -72$ mV when $K_o = 5$ mM (the mean value of three studies with cells isolated from cats, rabbits, and rats; refs. 7, 36, and 37). The rate of aldosterone secretion for each K_o is normalized by the rate for $K_o = 10$ mM (ref. 1; see Fig. 4). Open triangles indicate the corresponding levels of ^{45}Ca influx (ref. 2; see Fig. 4). (*C*) Voltage-dependent block of the T-type Ca channels by nitrendipine. The *Right Insets* show superimposed tail current measurements with and without 0.3 μM nitrendipine. The control records were fit by an exponential with a time constant of 5.8 ms. The records in drug (indicated by an asterisk) were fit by an exponential with time constants of 5.0 ms and 4.8 ms for $V_p = -110$ mV and −60 mV, respectively. The prepulse duration was 4.5 s for each control and 10 s in drug. Each current record was blanked for 450 μs after repolarizing the membrane. The relative amplitude of the slowly deactivating component of current is plotted vs. V_p. The solid curve through each set of data points indicates the least squares fit to the equation: $I/I_{max} = \{1 + \exp[(V_p - V_{1/2})/k]\}^{-1}$. For the curve through the control data, $V_{1/2} = -64.6$ mV and $k = 8.15$; in 0.3 μM nitrendipine, $V_{1/2} = -72.6$ mV and $k = 9.14$.

T-type Ca channels comes from studies with nitrendipine: nitrendipine blocks the T-type Ca channels and K^+-induced ^{45}Ca influx with similar potency. Fig. 3*C* shows the steady-state voltage dependence of nitrendipine block of the T-type Ca channels. The pulse protocol is shown in the *Left Inset* and it is the same as that used for Fig. 2*A*. The prepulse duration was 10 s with drug so that drug binding could equilibrate at each V_p. The *Right Inset* shows superimposed tail currents with and without 0.3 μM nitrendipine for two prepulse potentials. When $V_p = -110$ mV, there was little block of the T-type Ca channels, although the rate of deactivation was speeded by drug. When $V_p = -60$ mV, about two-thirds of the channels were inactivated in the absence of drug and block was much more potent. The voltage dependence of nitrendipine block is indicated by a plot of the relative amplitude of the slow component of tail current vs. V_p. Each datum point represents the mean of two experiments. The effect of 0.3 μM nitrendipine is to shift the availability curve to more negative potentials with little change in slope factor.

To compare nitrendipine block of the T-type Ca channels with block of K^+-induced ^{45}Ca influx, one must evaluate the effective binding constant for nitrendipine block of T-type Ca channel currents at any voltage (K_{eff}). This calculation is facilitated by use of the modulated receptor theory, which postulates that the affinity of nitrendipine for its binding site is modulated by channel gating (38, 39). This model has been used to quantitate the block of Na channels by local anesthetics and the block of L-type Ca channels by dihydropyridines (40–42). In these earlier studies, it was assumed that steady-state drug binding was to rested or inactivated channels. The extension of this theory to T-type Ca channels in adrenal glomerulosa cells is complicated by the finding that channels remain open in the steady state. It can be shown that the steady-state availability curve in drug (h_∞') is given by:

$$h_\infty' = (1 + D/K_R)/\{(1 - m_\infty^2)(1 + D/K_R) + m_\infty^2(1 + D/K_O) + [(1 - h_\infty)/h_\infty](1 + D/K_I)\}, \quad [1]$$

where K_R, K_O, and K_I are the dissociation constants for drug binding to the rested, open, and inactivated states, respectively; D is the drug concentration; and m_∞^2 and h_∞ describe the voltage dependence of activation and inactivation, as in Fig. 3*A*. It follows that $K_{eff} = [(1 - m_\infty^2)h_\infty/K_R + m_\infty^2 h_\infty/K_O + (1 - h_\infty)/K_I]^{-1}$.

K_R is calculated from the amount of block when $V_p = -110$ mV; the average value for two experiments was 13.4 μM. The more potent block observed at less negative values of V_p could be due to high-affinity binding to open or inactivated channels. Since the occupancy of the inactivated state is much greater than the occupancy of the open state for $V_p < -50$ mV, binding to the open state can be ignored unless $K_O << K_I$. It is unlikely that $K_O << K_I$ because block was not much more potent at more positive potentials, where occupancy of the open state is greater (unpublished results). Hence, Eq. **1** can be simplified to consider drug binding only to rested and inactivated states. K_I can be calculated from the data presented in Fig. 3*C* with use of the equation: $K_I = D/[(1 + D/K_R)\exp(-\Delta V/k) - 1]$, where ΔV is the voltage difference between the midpoint of the availability curves with and without drug and k is the mean slope factor of the availability curves (40). From the data used for Fig. 3*C*, $K_I = 190$ nM. In one experiment with nimodipine, we obtained similar results, with $K_I = 144$ nM. Similar effects of diphydropyridines on T-type Ca channels have been found in cell lines derived from anterior pituitary cells and aortic smooth muscle (17).

The membrane potential should be -65 mV in 8 mM K^+ and -76 mV in 3.5 mM K^+. The predicted values for K_{eff} at these two voltages are 0.54 μM and 1.7 μM, respectively. Nitrendipine blocks ^{45}Ca influx induced by 8 mM K^+ with an $IC_{50} = 0.45$ μM (ref. 1; see figure 2) and the block of basal secretory activity is much weaker (ref. 2; see table I).

FIG. 4. AII increases T-type Ca channel currents. Tail currents were measured at -75 mV after a 40-ms test pulse to $+10$ mV. Each current record was blanked for 500 μs after repolarizing the membrane potential.

Nitrendipine also blocks the AII-induced influx of ^{45}Ca into adrenal glomerulosa cells (1, 2). This result suggests that AII modulates a voltage-gated Ca channel. Fig. 4 shows that current through the T-type Ca channels is increased by 10 nM AII. Superimposed tail current measurements are shown. Each tail current measurement was fit by a single exponential and the asterisk indicates the current recorded after a 20-s exposure to AII. The amplitude of the exponential was increased by about 50% and the time constant of decay was increased from 8.75 to 11.5 ms. Similar results were obtained in three of four similar experiments. The effect of AII on channel gating was not analyzed in detail because the effect was very transitory, lasting, at most, several minutes.

DISCUSSION

Bovine adrenal glomerulosa cells have two components of Ca channel tail current that we have attributed to two distinct populations of Ca channels (see Figs. 1 and 2). This interpretation is supported by the findings that the two components of current have different activation, inactivation, and deactivation kinetics and different susceptibilities to modification by BAY K 8644 and to rundown. Studies in other types of excitable cells have shown that two similar components of Ca channel current are associated with distinctly different patterns of single channel activity (31, 32, 43). Previous studies with adrenal glomerulosa cells also provide evidence for two populations of Ca channels (2). The L-type Ca channels account for the high-affinity binding sites for [^{3}H]nitrendipine and the enhancement of Ca influx by BAY K 8644 (1–4). The T-type Ca channels account for the stimulation of Ca influx by small depolarizations from rest (see below) and the Ca currents reported in a recent voltage clamp study with rat adrenal glomerulosa cells (44). L-type Ca channels were not reported in the studies with rat cells, but it is possible that these channels "washed out" during dialysis of the cytoplasm. We have found the washout effect to be severe, even when we used pipette solutions that minimize the effect in other types of cells (16, 26). The problem may be severe because adrenal glomerulosa cells are small (8–12 μm in diameter), so dialysis of the cytoplasm may be more complete than in larger cells. It is possible that we have significantly underestimated the magnitude of L-type Ca currents in intact cells.

Stimulus–secretion coupling in adrenal glomerulosa cells is unusually sensitive to small increases in plasma K^+, apparently because Ca influx is stimulated at lower K_o than in most other types of cells. Our studies suggest that the high sensitivity to changes in plasma K^+ occurs because maintained Ca influx through T-type Ca channels can be adequate

to stimulate aldosterone secretion. Under physiological conditions, the membrane potential ranges from −80 to −50 mV (7, 9, 36, 37). In this voltage range, the T-type Ca channels activate to a much greater extent than the L-type Ca channels and inactivation of the T-type channels does not go to completion (see Figs. 1 and 3*A*). Since there should be steady-state current through the T-type Ca channels, the description of these channels as transient is misleading. The probability that a T-type Ca channel will be open at −60 mV is only ≈0.01, but the surface-to-volume ratio in adrenal glomerulosa cells is large and the Ca influx necessary to trigger aldosterone secretion can occur over many minutes. Hence, it is probable that extremely small Ca currents can mediate stimulus-secretion coupling. The idea that there are maintained currents through T-type Ca channels is supported by the recent finding in this laboratory that 3 nM atriopeptin blocks current through these channels and blocks K^+-stimulated aldosterone secretion (45). We have also found evidence for steady-state current through T-type Ca channels in cell lines derived from anterior pituitary cells and vascular smooth muscle (16, 17).

In some other types of endocrine cells and vascular smooth muscle, K^+-induced Ca influx is associated with L-type Ca channels because it is blocked by dihydropyridines with high affinity (14–17). It is possible that some of the K^+-induced Ca influx is through L-type Ca channels in adrenal glomerulosa cells, but our results suggest that most of the influx is through T-type channels for $K_o < 12$ mM. Steady-state current through L-type Ca channels was maximal at ≈−25 mV in our studies (see Figs. 1 and 2) and at this potential ≈80% of the channels are inactivated. In other tissues, nitrendipine block of L-type Ca channels is very potent when most channels are inactivated (15, 41, 42). The maximal current through L-type channels could occur at more negative potentials under physiological conditions, but the low potency of nitrendipine block of Ca influx requires that the voltage dependence of channel activation shifts to more negative potentials much more than that for channel inactivation. This seems unlikely. Furthermore, the voltage dependence of activation of L-type Ca channels in glomerulosa cells is similar to that in some other endocrine cells, so there is little reason to expect Ca influx through L-type channels at unusually negative potentials in glomerulosa cells (see refs. 16, 46, and 47 for activation curves in anterior pituitary cells, pancreatic beta cells, and adrenal chromaffin cells, respectively). Ca entry through L-type Ca channels may be important when adrenal glomerulosa cells are depolarized beyond −50 mV, especially when there is electrical spiking activity (37).

The modulation of T-type Ca channels by AII is especially interesting because there are few reports of neurotransmitters or autacoids affecting this channel type (30, 48, 49). In contrast, L-type Ca channels are modulated by many agents (50), including AII (51, 52). The effect of AII on the T-type Ca channels never lasted more than a few minutes. The effect may have been brief because it was mediated by a second messenger that was rapidly dialyzed from the cell. For example, the effects on T-type Ca channels could be secondary to the formation of one or more inositol polyphosphates (8, 20, 53, 54). This possibility is attractive because inositol polyphosphates are thought to stimulate Ca influx in many types of endocrine cells (55).

This work was supported in part by National Institutes of Health Grant DK19813 to P.Q.B and H.R.

1. Kojima, K., Kojima, I. & Rasmussen, H. (1984) *Am. J. Physiol.* **247,** E645–E650.
2. Kojima, I., Kojima, K. & Rasmussen, H. (1985) *J. Biol. Chem.* **260,** 9171–9176.
3. Kojima, I., Kojima, K. & Rasmussen, H. (1985) *J. Biol. Chem.* **260,** 9177–9184.
4. Aguilera, G. & Catt, K. J. (1986) *Endocrinology* **118,** 112–118.
5. Schiebinger, R. J., Braley, L. M., Menachery, A. & Williams, G. H. (1986) *J. Endocrinol.* **110,** 315–325.
6. Braley, L. M., Menachery, A. I., Brown, E. M. & Williams, G. H. (1986) *Endocrinology* **119,** 1010–1019.
7. Quinn, S. J., Cornwall, M. C. & Williams, G. H. (1987) *Endocrinology* **120,** 903–914.
8. Guillemette, G., Baukal, A. J., Balla, T. & Catt, K. J. (1987) *Biochem. Biophys. Res. Commun.* **142,** 15–22.
9. Foster, R., Lobo, M. V., Rasmussen, H. & Marusic, E. T. (1982) *FEBS Lett.* **149,** 253–256.
10. Kojima, I., Kojima, K. & Rasmussen, H. (1985) *Biochem. J.* **228,** 69–76.
11. Hyatt, P. J., Tait, J. F. & Tait, S. A. (1986) *Proc. R. Soc. London Ser. B* **227,** 21–42.
12. Foster, R., Lobo, M. V., Rasmussen, H. & Marusic, E. T. (1981) *Endocrinology* **109,** 2196–2201.
13. Capponi, A. M., Lew, P. D., Jornot, L. & Valloton, M. B. (1984) *J. Biol. Chem.* **259,** 8863–8869.
14. Bean, B. P., Sturek, M., Puga, A. & Hermsmeyer, K. (1986) *Circ. Res.* **59,** 229–235.
15. Kunze, D. L., Hamilton, S. L., Hawkes, M. J. & Brown, A. M. (1987) *Mol. Pharmacol.* **31,** 401–409.
16. Cohen, C. J. & McCarthy, R. T. (1987) *J. Physiol. (London)* **387,** 195–225.
17. McCarthy, R. T. & Cohen, C. J. (1987) *Biophys. J.* **51,** 224 (abstr.).
18. Triggle, D. J. & Janis, R. A. (1984) in *Modern Methods in Pharmacology*, eds. Back, N. & Spector, S. (Liss, New York), pp. 1–28.
19. Foster, R. & Rasmussen, H. (1983) *Am. J. Physiol.* **245,** E281–E287.
20. Kojima, I., Kojima, K., Kreuter, D. & Rasmussen, H. (1984) *J. Biol. Chem.* **259,** 14448–14457.
21. Fakunding, J. L., Chow, R. & Catt, K. J. (1979) *Endocrinology* **105,** 327–333.
22. Cohen, C. J., McCarthy, R. T., Barrett, P. Q. & Rasmussen, H. (1987) *Biophys. J.* **51,** 224 (abstr.).
23. Marty, A. & Neher, E. (1983) in *Single-Channel Recording*, eds. Sakmann, B. & Neher, E. (Plenum, New York), pp. 107–122.
24. Colquhoun, D. (1971) *Lectures on Biostatistics* (Oxford Univ. Press, London), p. 263.
25. Matteson, D. R. & Armstrong, C. M. (1986) *J. Gen. Physiol.* **87,** 161–182.
26. Cota, G. (1986) *J. Gen. Physiol.* **88,** 83–105.
27. Carbone, E. & Lux, H. D. (1987) *J. Physiol. (London)* **386,** 547–570.
28. Bean, B. P. (1985) *J. Gen. Physiol.* **85,** 1–30.
29. Bossu, J. L., Feltz, A. & Thomann, J. M. (1985) *Pflügers Arch.* **403,** 360–368.
30. Narahashi, T., Tsunoo, A. & Yoshii, M. (1987) *J. Physiol. (London)* **383,** 231–249.
31. Nowycky, M. C., Fox, A. P. & Tsien, R. W. (1985) *Nature (London)* **316,** 440–443.
32. Nilius, B., Hess, P., Lansman, J. B. & Tsien, R. W. (1985) *Nature (London)* **316,** 443–446.
33. Fedulova, S. A., Kostyuk, P. G. & Veselovsky, N. S. (1985) *J. Physiol. (London)* **359,** 431–446.
34. Yatani, A., Seidel, C. L., Allen, J. & Brown, A. M. (1987) *Circ. Res.* **60,** 523–533.
35. DeRiemer, S. A. & Sakmann, B. (1986) *Exp. Brain Res.* **14,** 139–154.
36. Matthews, E. K. & Saffran, M. (1973) *J. Physiol. (London)* **234,** 43–64.
37. Natke, E., Jr., & Kabela, E. (1979) *Am. J. Physiol.* **237,** E158–E162.
38. Hille, B. (1977) *J. Gen. Physiol.* **69,** 497–515.
39. Hondeghem, L. M. & Katzung, B. G. (1977) *Biochim. Biophys. Acta* **472,** 373–398.
40. Bean, B. P., Cohen, C. J. & Tsien, R. W. (1983) *J. Gen. Physiol.* **81,** 613–642.
41. Bean, B. P. (1984) *Proc. Natl. Acad. Sci. USA* **81,** 6388–6392.
42. Sanguinetti, M. C. & Kass, R. S. (1984) *Circ. Res.* **55,** 336–348.
43. Carbone, E. & Lux, H. D. (1987) *J. Physiol. (London)* **386,** 571–601.
44. Matsunaga, H., Maruyama, Y., Kojima, I. & Hoshi, T. (1987) *Pflügers Arch.* **408,** 351–355.
45. McCarthy, R. T., Rasmussen, H. & Barrett, P. Q. (1988) *Biophys. J.* **53,** 557 (abstr.).
46. Rorsman, P. & Trube, G. (1986) *J. Physiol. (London)* **374,** 531–550.
47. Fenwick, E. M., Marty, A. & Neher, E. (1982) *J. Physiol. (London)* **331,** 599–635.
48. Dolphin, A. C. & Scott, R. H. (1987) *J. Physiol. (London)* **386,** 1–17.
49. Marchetti, C., Carbone, E. & Lux, H. D. (1986) *Pflügers Arch.* **406,** 104–111.
50. Reuter, H. (1983) *Nature (London)* **301,** 569–574.
51. Mironneau, J., Mironneau, C., Grosset, A., Hamon, G. & Savineau, J.-P. (1980) *Eur. J. Pharmacol.* **68,** 275–285.
52. Kass, R. S. & Blair, M. L. (1981) *J. Mol. Cell. Cardiol.* **13,** 797–809.
53. Enyedi, P., Buki, B., Mucsi, I. & Spat, A. (1985) *Mol. Cell. Endocrinol.* **41,** 105–112.
54. Smith, J. B. (1986) *Am. J. Physiol.* **250,** F759–F769.
55. Putney, J. W., Jr. (1986) *Annu. Rev. Physiol.* **48,** 75–88.